Size-Dependent Crystal Growth—A Manifestation of Growth Rate Dispersion in the Potassium Alum-Water System

Growth of potassium alum crystals was characterized by the advance rates of crystals on the leading edge of population distributions and by the advance rates of the modes of these distributions. Growth rates of crystals on the leading edge appeared to follow size-dependent kinetics, but the observed spread of the distribution about the average size was much greater than would be expected from size-dependent growth alone. The spread of the distribution was correlated with the extent of growth determined from the net advance of the average crystal size. These quantitative and qualitative results show that what has often been referred to as size-dependent growth is in fact a manifestation of growth rate dispersion.

M. W. GIROLAMI

and R. W. ROUSSEAU

Department of Chemical Engineering,
North Carolina State University
Raleigh, NC 27695

SCOPE

Both growth rate dispersion and size-dependent growth have been observed to occur under specific conditions in the aqueous potassium alum system. Data on this and other systems often exhibit characteristics of these growth anomalies, and it has been unclear to what extent each mechanism of growth rate variability contributes to or controls the measured growth kinetics and the development of a crystal size distribution. The importance of being able to identify the correct growth mechanism is based on the role it plays in obtaining crystallization kinetics from experimental or operating data, and on the use of such data for the design of large-scale crystallizers.

The analysis of crystal size distributions to determine nucleation and growth kinetics requires a knowledge of the relationship of growth rate to crystal size. Such analyses are simple if all crystals in a population grow at identical rates and have no dependence on size. Deviations from invariant crystal growth have been noted for quite some time, but it is only recently that such deviations have been attributed to growth rate dispersion rather than size-dependent growth. Distinction between these two sources of anomalous growth is difficult because their effect on a crystal size distribution is the same: they cause a distribution to spread during growth and, for perfectly mixed crystallizers, they indicate higher nuclei population densities than would be expected for invariant crystal growth. This similarity can cause crystal size distributions obtained through one of the anomalous growth mechanisms to be misinterpreted as the result of the other. In such cases, using correlations based on the incorrect mechanism could lead to a serious errors in scale-up and design.

The objectives of this study were to characterize the effects of growth rate variability on the form of developing crystal size distributions of both large and small potassium alum crystals, to separate the effects of size-dependency and growth rate dispersion, and to develop correlations of the observed behavior that could be used to analyze potassium alum systems and give qualitative guidance to the behavior of other systems.

CONCLUSIONS AND SIGNIFICANCE

Growth rate variability, whether the result of size-dependent growth or growth rate dispersion, causes an increase in the spread of the developing crystal size distribution. As a measure of the growth rate variability in the population of nuclei formed by initial breeding, the variance of the population was determined as a function of the extent of growth of the crystals. Before growth, the estimated mean size of these crystals was 5 μm and the size variance in the distribution was 7.3 μm^2. The advance rate of the average crystal size was determined to be independent of the average size and proportional to the relative supersaturation to the 1.6 power. On the other hand, following the growth of crystals on the leading edge of the population formed by initial breeding showed that their growth was proportional to the relative supersaturation but dependent on size to the 0.4 power.

Using the apparent relationship of growth to size obtained from following the growth of crystals on the leading edge of

Correspondence concerning this paper should be addressed to R. W. Rousseau.

the population obtained from initial breeding, an estimate of the variance of the distribution brought about by size-dependent growth was obtained. The measured size variance was found to be much greater than that estimated from the effect of size-dependent growth alone. Similar results were also obtained for the growth of narrow distributions of seed crystals that had initial mean sizes before growth of 275.0 and 327.5 μm.

These results show that the apparent relationship between growth rate and crystal size that has been observed for potassium alum is a manifestation of growth rate dispersion; moreover, it is likely that size-dependent growth kinetics reported for other systems is the result of this phenomenon. The reason for the apparent relationship between growth and size is as follows: with growth rate dispersion, crystals grown in a batch system are classified into sizes by their growth rates, and following the growth of crystals at a given size one observes the effects of growth rate dispersion rather than size-dependent kinetics.

INTRODUCTION

There are important and numerous exceptions, particularly at low supersaturation, to the simple picture of size-independent crystal growth embodied in the ΔL law (McCabe, 1929). These exceptions have been observed since the application of microscopy and electronic particle counters to the study of growth of small crystals. Growth rate dispersion and size-dependent crystal growth are deviations from the ΔL law which differ in mechanism but give similar characteristics to crystal size distributions within which they occur.

Growth rate dispersion refers to the exhibition of different growth rates by crystals, even though they have the same size and are exposed to identical conditions for growth. This phenomenon may include zero growth and abrupt changes in growth rates of individual crystals, and the dispersion in growth rates leads to a broadening of the size distribution of a crystal population. Size-dependent growth refers to deviations from the ΔL law that occur when growth rates are a function of crystal size. This condition can also lead to a broadening of a size distribution if the population of crystals is not monosized.

Plots of the log of crystal population density vs. size for crystals obtained from a perfectly mixed, continuous (MSMPR) crystallizer with a clear feed often exhibit pronounced upward curvature at small crystal sizes and linearity at large sizes, whereas the ΔL law requires linearity over the entire size range. Such observations have been explained by high nucleation rates and size-dependent growth of crystals in the smallest size range (Garside and Davey, 1980). Independent measurements of growth kinetics from seeded batch crystallizers indicate that the growth of secondary nuclei smaller than 100 μm is strongly size-dependent (Garside and Davey, 1980; Garside and Jancic, 1976; Rousseau et al. 1979). However, this explanation of the observations has not been satisfying because a single mechanism to explain both size-dependent growth kinetics of small crystals and size-independent kinetics of large crystals has been accepted.

White and Wright (1971) first characterized the effects of growth rate dispersion on a population of sucrose crystals by correlating the population variance σ_L^2 about a mean size L with the extent of growth of the crystals in a seeded batch crystallizer. The original crystals were of uniform size and the mean of the crystal size distribution was used as a measure of the extent of growth. The relationship between the variance and extent of growth was linear and had slope p, which was proportional to the magnitude of the spread of the distribution. Growth rate dispersion for sucrose was found to be significant (p = 67 μm), but the same authors found negligible dispersion (p = 1 μm) for aluminum trihydroxide. The slope p did not depend on the initial seed size (10 to 500 μm) or the stirring rate in the crystallizer, and it decreased when growth rate and impurity concentration increased or when brief intervals of dissolution occurred. Janse and deJong (1976, 1979) found growth rate dispersion important in the growth of large potassium dichromate and potassium alum crystals, and demonstrated that this phenomenon could account for upward curvature of the MSMPR crystallizer population density plots mentioned earlier. They concluded that growth rate dispersion could provide an explanation of what had been considered to be size-dependent growth, but that both phenomena could occur simultaneously; the occurrence of growth rate dispersion does not rule out the possibility that single crystal growth may be size-dependent.

Recent microscopic studies of individual secondary nuclei have observed growth rate dispersion and size-dependent growth directly (Garside and Larson, 1978; Berglund and Larson, 1982). Garside et al. (1979) and Garside (1979) report that two types of potassium alum secondary nuclei form after gentle contact of a seed crystal. Those less than 4 μm in size were created in larger numbers and were formed even if the solution was undersaturated. The number of such nuclei was relatively independent of supersaturation. These nuclei grew more slowly than larger ones, and in some cases did not grow at a measurable rate. The number and size of nuclei between 4 and 50 μm in size increased as supersaturation was increased. Large crystals were not formed in saturated or undersaturated solution, but in supersaturated solutions tended to grow more rapidly than small crystals. Contact nuclei of citric acid monohydrate, on the other hand, showed growth rate dispersion but no size-dependent growth (Berglund and Larson, 1982). Very slow or zero growth rates for small secondary nuclei have been reported by Bujac (1976), who worked with aqueous solutions of pentaerythritol, and by van't Land and Wienk (1976) in their studies on sodium chloride. Several types of nuclei were distinguished by their size, shape, and individual growth behavior.

Randolph and White (1977) defined a growth diffusivity which they used to model growth rate dispersion. Their model resulted in a constant value of p. Berglund and Larson (1984) on the other hand used distributions of growth rates and initial crystal size to model growth rate dispersion of citric acid. Values of p resulting from this model are not constant.

The objective of this research was to determine the relative magnitudes of growth rate dispersion and size-dependent growth, and the effects of these growth anomalies on the development of a characterized crystal size distribution. Garside and Davey (1980) used both growth anomalies to explain observed behavior in the crystallization of potassium alum in perfectly mixed, continuous crystallizers. It is by no means clear to what extent each contributes to or controls crystal growth, and this information is critical in modeling nucleation and growth kinetics for crystallizer simulation. Nucleation kinetics are evaluated on an effective basis—that is, the rate at which nuclei grow into an observable size range—and failure of a large fraction of nuclei to grow at significant rates is a troublesome feature of modeling systems with growth rate dispersion.

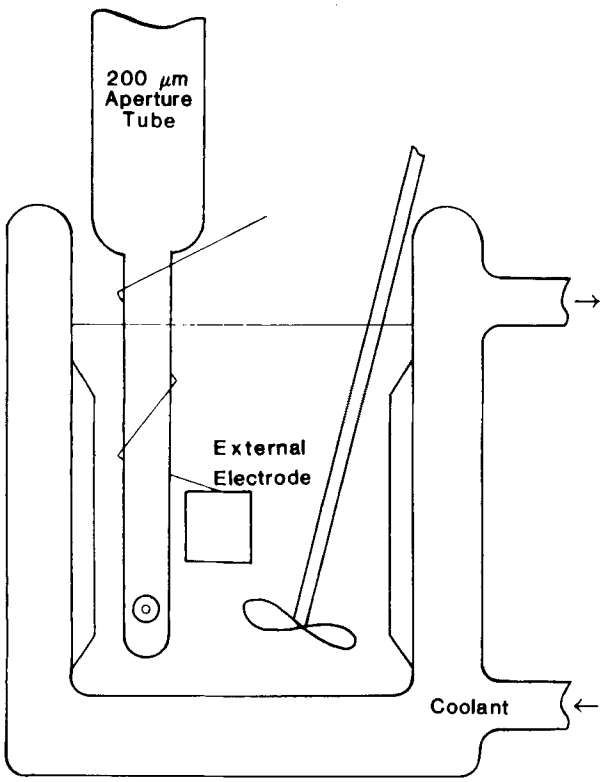

Figure 1. Experimental batch crystallizer.

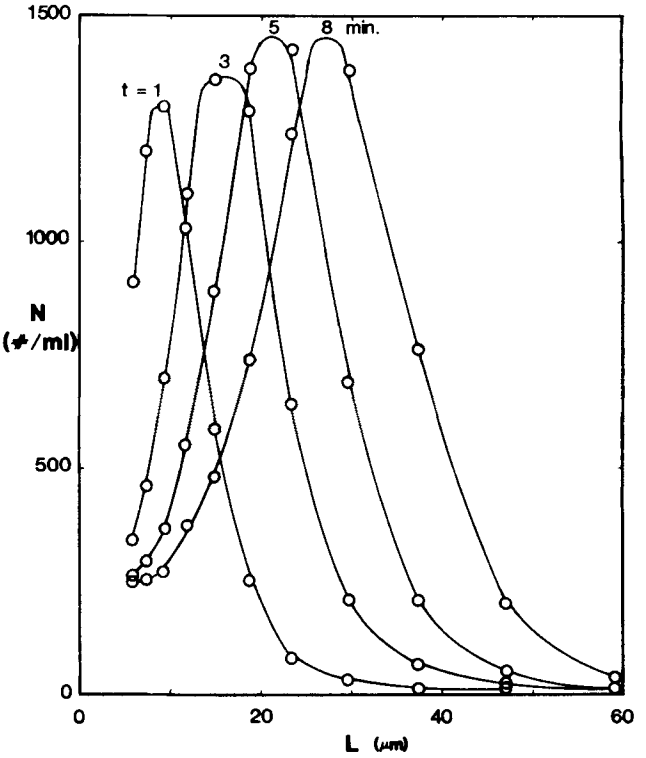

Figure 3. Typical number distribution transients used in this study.

EXPERIMENTAL

By seeding a supersaturated potassium alum solution, the growth of two populations of crystals—large seed crystals and small crystals resulting from initial breeding—could be measured and compared. Since a narrow size distribution of large numbers of small crystals could be obtained by initial breeding, these crystals were considered ideally suited for the proposed study. In addition to having a narrow initial distribution, crystals produced by initial breeding may be presumed to be well-formed in comparison to those from contact nucleation, and therefore observations of growth behavior are not confounded with variations in crystal structure due to the nucleation mechanism. Potassium alum was selected for these experiments because both size-dependent growth and growth rate dispersion have been used to explain its behavior in MSMPR crystallizers, and because it grows by a dislocation mechanism at low to moderate supersaturation (Bennema, 1967; Van Enckevort and Van der Linden, 1979).

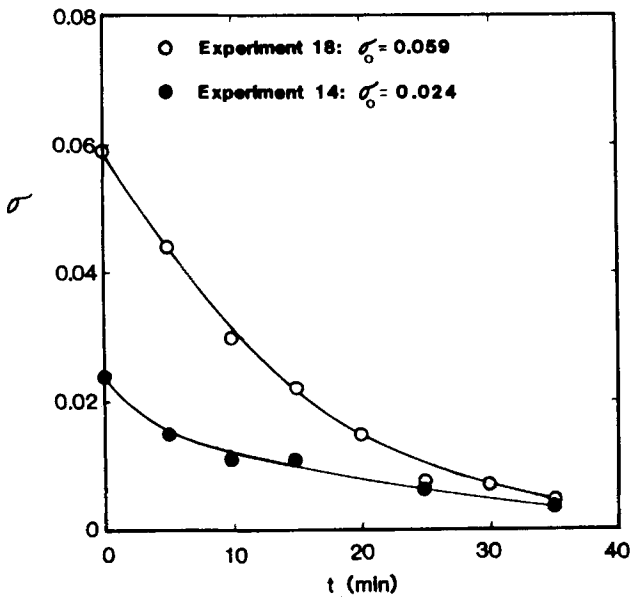

Figure 2. Measured desupersaturation rates in representative experiments.

These experiments employed a constant temperature batch crystallizer shown in Figure 1. It is a jacketed glass vessel made with 3 baffles having a 200 ml capacity. The crystallizer temperature was maintained at 29.4 ± 0.1°C in all experiments. All solutions were obtained by dilution of aliquots taken from one master solution. Deionized water and ACS Certified reagent grade potassium alum were used in all preparations. Once the preheated and filtered solution was poured into the crystallizer, stirring was begun and the system was cooled to the desired supersaturation and temperature.

Seed crystal samples were taken from two carefully sieved populations and were 250–300 μm or 300–355 μm in size. One population consisted of well-formed octahedral crystals that had been partially dissolved and regrown at 36°C. The second population was made up of spherical crystals prepared by abrasion of octahedrons. This was accomplished by vigorously stirring an equilibrated 40% solids slurry of crystals for 19 h at 29°C. Both populations were finally rinsed quickly with acetone upon separation from solution by filtration and allowed to air-dry before sieving into the desired fractions. Between 0.27 and 4.35 g of these large crystals was used to seed 150 ml of the supersaturated solution held in the batch crystallizer. Variations in mass of seed crystals were used to generate appropriate numbers of nuclei.

A calibrated refractometer was used to measure the concentration of potassium alum in aqueous solutions. A precision of ±0.05 g alum/100 g solution could be obtained with this instrument.

A TA II Coulter Counter, fitted with a 200 μm aperture tube, was employed to monitor crystal size distribution. This aperture allowed detection of crystals having equivalent diameters between 4 and 80 μm. Particle counts in the lowest channel, however, were confounded by electrical noise and were unreliable. Because the Coulter Counter relates crystal size to the diameter of an equivalently size sphere, a correction must be made in the data to account for the octahedral symmetry of potassium alum. The edge length L between (111) faces of the octahedron

was determined by equating volumes of a sphere having a diameter L_s to the volume of an octahedron to obtain $L = 1.036\ L_s$.

Experimental Measurements

Throughout a crystal growth experiment, usually every three to four minutes after addition of seed crystals, samples of solution were withdrawn from the batch crystallizer for measurement of both solute concentration and small crystal size distribution. Figure 2 shows measured rates of desupersaturation for two representative experiments in which the solutions had different initial supersaturations, but were each seeded with crystals having a surface area of 165 cm^2. The smoothed data were used to estimate an average supersaturation at which a pair of transient crystal size distributions were measured.

Examples of the crystal size distributions measured in an experiment are shown in Figure 3. These data have been corrected by subtraction of background counts. The first moment of each distribution is the mean size or centroid of the distribution,

$$\bar{L} = \sum N_i L_i / \sum N_i \tag{1}$$

where N_i is the number of crystals/mL in channel i of a mean size L_i. The distribution spread can be determined as the size variance by

$$\sigma_L^2 = \sum N_i (L_i - \bar{L})^2 / \sum N_i \tag{2}$$

Another useful parameter in the characterization of the distribution is the moment coefficient of kurtosis, a_4, which is a standard measure of distribution height or peakedness.

$$a_4 = (1/\sigma_L^4) \sum N_i (L_i - \bar{L})^4 / \sum N_i \tag{3}$$

Growth Rate Determinations

Crystal growth rates characterized by displacement of a crystal size distribution can be calculated in two ways: displacement rate of the centroid of the distribution or displacement rate of a fraction of oversize crystals. If a centroid displacement $\Delta\bar{L} = \bar{L}_2 - \bar{L}_1$ occurs in a time interval Δt, the growth rate using the first method of determination is

$$\bar{G} = \Delta\bar{L}/\Delta t \tag{4}$$

The second growth rate determination was first proposed by Misra and White (1971). This method, described in detail elsewhere (Garside and Jancic, 1979), requires that the total number of crystals in the distribution remain constant and that growth rate dispersion not occur. Growth rates are calculated by

$$G = \Delta L/\Delta t \tag{5}$$

where Δt is the time interval between measurements of the crystal size distribution. In this study, displacements between oversize fractions less than those corresponding to mean sizes were used in Eq. 5 to calculate growth rates. This was done to avoid potential errors associated with including crystals formed by nucleation during the experiment, and to insure that the growth rates obtained were those representing crystals on the leading edge of the distribution.

Growth rates of seed crystals were calculated from Eq. 4 using the original mass of crystals m_o, final mass of crystals m_f, and the original average crystal size $\bar{L}_o$ to estimate ΔL:

$$\Delta L = \bar{L}_f - \bar{L}_o = [(m_f k_{vo}/m_o k_{vf})^{1/3} - 1]\bar{L}_o \tag{6}$$

This relationship was obtained by setting the original number of seed crystals equal to the final number after growth n_c, solving for $\bar{L}_f$, and subtracting $\bar{L}_o$ to obtain ΔL; n_c is given by

$$n_c = m/(k_v \rho_c \bar{L}^3) \tag{7}$$

RESULTS

Growth of Crystals Within a Distribution

Potassium alum growth rates obtained by the Misra and White method (1971) are plotted in Figure 4 for three potassium alum

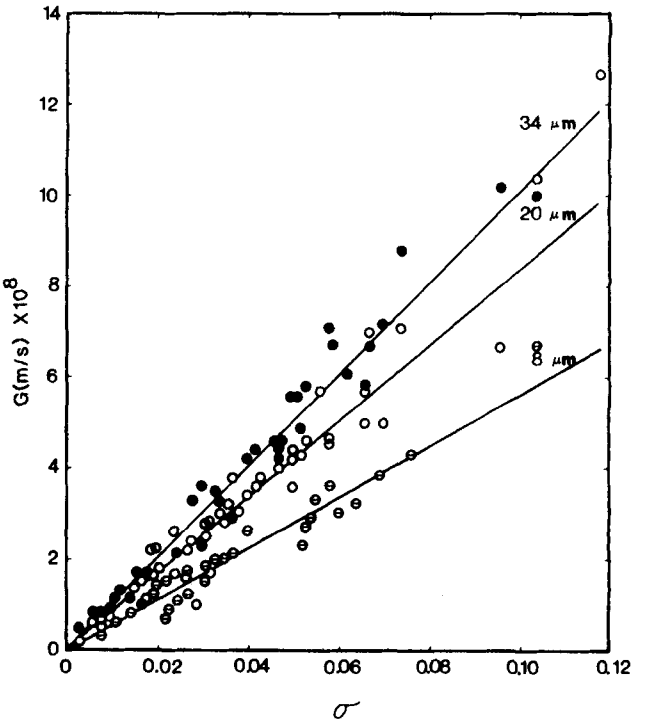

Figure 4. Growth rates of small potassium alum crystals as functions of supersaturation and size.

crystal sizes: 8, 20 and 34 μm. These sizes are averages of initial and final values used to determine ΔL within a specific size range. As can be seen, measured growth rates increase as crystal size increases, corresponding to the phenomenon of size-dependent growth. Although the relationship between growth rate and supersaturation appears linear, a power law function was tested in correlating the kinetic data:

$$G = K_G \sigma^n \tag{8}$$

Table 1 summarizes correlations obtained by linear regression, and also gives 95% confidence intervals on K_G and n. As n ranges from 1.00 to 1.12, the departure from a linear dependence of growth rate on supersaturation is small. It is of interest to note that n increases as size decreases, although the trend is not significant at the 95% confidence levels.

In the Burton-Cabrera-Frank (BCF) theory (1951), crystal growth rate is given by

$$G = C(\epsilon\sigma^2/\sigma_1') \tanh(\sigma_1'/\epsilon\sigma) \tag{9}$$

where ϵ is screw dislocation activity and σ_1' is system-dependent and inversely proportional to temperature. The form of the functional dependence of growth rate on supersaturation depends on the ratio $(\sigma_1'/\epsilon\sigma)$. If this ratio is greater than about 5, $\tanh(\sigma_1'/\epsilon\sigma)$ approaches unity and the growth rate becomes a parabolic function of supersaturation; on the other hand, if the ratio is less than

TABLE 1. POWER LAW OF POTASSIUM ALUM GROWTH RATES

Crystal Size μm	Correlation		95% Confidence Limits on Coefficient K_G
8	$G \times 10^8 = 80$	1.12 ± 0.13	51–125
20	$G \times 10^8 = 96$	1.06 ± 0.07	74–124
34	$G \times 10^8 = 97$	1.00 ± 0.07	76–126

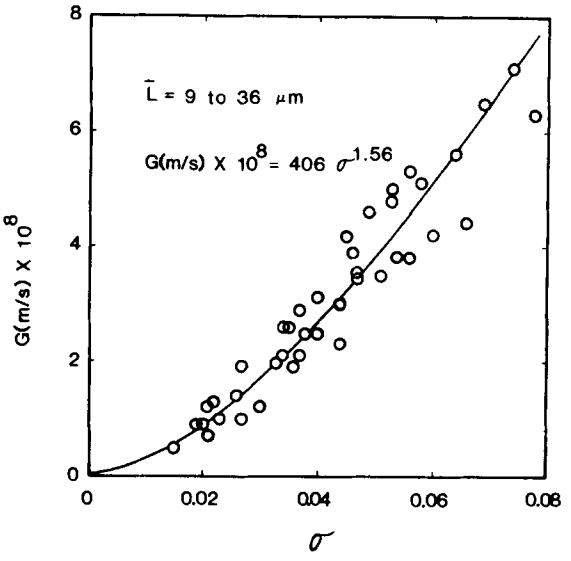

Figure 5. Advance (growth) rates for the modes of potassium alum crystal size distributions.

about 0.05, the functional relationship becomes linear. It is clear then that n must be between 1 and 2, and, at some intermediate range of supersaturation, the value of n may depend on the screw dislocation activity.

Consider now the population of crystals formed by initial breeding in a batch crystallizer. Assume that they are initially at approximately the same size when they are formed. The BCF theory says that those crystals with higher dislocation activities will grow more rapidly, and at some subsequent time be larger in size than crystals with lower dislocation activities. If the growth rates of crystals in various size ranges are examined at conditions corresponding to the intermediate supersaturation range referred to earlier, a modest dependence of n on size might be expected, as was noted for the present data.

A power-law model was fit to all growth rate data obtained on the small crystals from initial breeding to obtain

$$G \times 10^8 = 25\, L^{0.40}\sigma \tag{10}$$

where growth rate G is in m/s and L is in μm. The 95% confidence limits on the coefficient are ±10, and on the order the 95% confidence limits are ±0.13. Nineteen experiments provided 140 data points for the development of Eq. 10. Growth rate dependence on size and supersaturation was the same, regardless of whether crystals were produced from well-formed or spherical seeds. As a result, growth kinetic data have been combined and will not be treated separately.

To compare the growth behavior of these crystals, whose origins are initial breeding, with those whose origins are contact nucleation, the data of Garside and Jancic (1976) were compared with those obtained in this study. In the work by Garside and Jancic, growth kinetics of small potassium alum crystals at 30°C were obtained from two sources: both dried crystals and liquid samples containing small collision nuclei were taken from a cooling MSMPR crystallizer. Also, small crystals were obtained by milling larger ones. No growth rate differences between these crystals were detected. Garside and Jancic seeded a batch crystallizer with crystals between 3 and 70 μm, and only a small surface area was introduced for growth so that supersaturation remained relatively constant in an experiment.

Garside and Jancic also found a linear relationship between crystal growth rate and supersaturation, and observed size-dependent growth kinetics. Correlation of their data gave the power-law relationship

$$G \times 10^8 = 26\, L^{0.49}\sigma \tag{11}$$

The 95% confidence limits are ±5 for the coefficient and ±0.07 on the order. Data for sizes less than 8 μm were not included in the analysis as they are outside the range of this study.

The similarities in Eqs. 10 and 11 are striking. The orders with respect to relative supersaturation are 1.0 in both, and the coefficient and order with respect to size agree closely. As has been said, the source of the observed size-dependent kinetics up to this point remains indeterminant.

Advance Rate of Distribution Mode

In this section, the growth kinetics of the entire crystal size distribution were determined using the centroid displacement method discussed earlier. The transient distributions used in this analysis were those that exhibited peaks indicating that the smaller sizes in the distribution were within the detection limits of the particle size analyzer. Additionally, a small correction was made in the particle counts in the trailing tail of the distribution by graphically extrapolating a plot of the distribution based on several data points in the region of the mode. This allowed estimation of revised particle counts in the small channel sizes, which eliminated contamination of the data by nucleation that may have occurred during an experiment.

Overall crystal distribution growth rates $\bar{G}$ were determined and are plotted against σ in Figure 5. These data were obtained for mean sizes between 9 and 36 μm. Within the accuracy of these data, there is no detectable dependence of distribution growth rate on mean size. The relationship between G and supersaturation is distinctly nonlinear, and was correlated by the expression

$$G \times 10^8 = 406\, \sigma^{1.56} \tag{12}$$

The units for G are m/s. The 95% confidence limits for the coefficient times 10^8 are 255 to 646, and ±0.14 for the order; the correlation coefficient is 0.963.

The order with respect to the relative supersaturation, 1.56, is larger than the orders found for 8, 20 and 34 μm potassium alum crystals growing on the leading edge of the crystal size distribution (Table 1). This difference must result from all crystals in the distribution contributing to the determination of $\bar{L}$ and $\bar{G}$. As has been discussed, these crystals exhibit a range of growth rates and varying supersaturation dependence. Recall that the order of dependence on supersaturation tended to increase as the screw dislocation activity decreased, and following the logic presented earlier for systems of the kind examined here, crystals in the smaller size ranges would be expected to have lower screw dislocation activities. This suggests that inclusion of large numbers of slow-growing, and therefore small, crystals in the trailing edge of the distribution in these calculations of growth rate is responsible for the increase in order shown in Eq. 12. Such an argument means that the order reflects the distribution of crystal growth rates within a population and that the source of these different growth rates is a frequency distribution of screw dislocation activities.

Influence of Size-Dependent Growth on Crystal Size Distribution Variance

Factors that influence the size variance of the crystal size distribution will be considered in this section. First, an estimate of the potential contribution by size-dependent growth will be made and evaluated. For this purpose, the net size variance function σ_{Ln}^2 and net growth $\bar{L}_n$ (also referred to as extent of

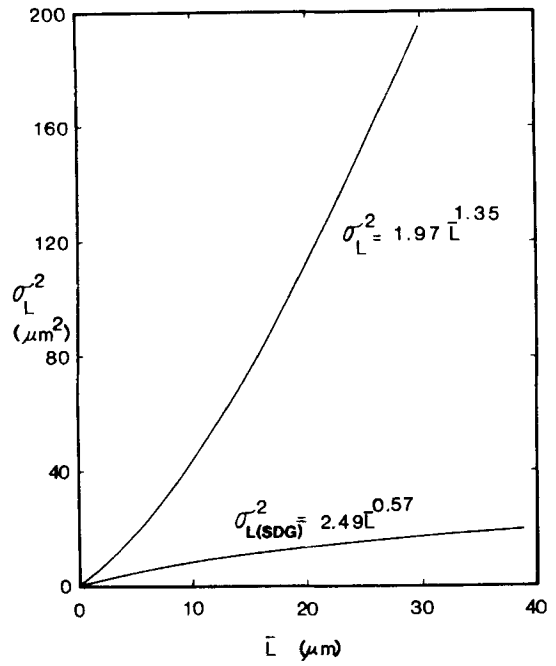

Figure 6. Comparison of dependence of size variance on extent of growth determined experimentally for small potassium alum crystals with that estimated assuming size-dependent growth kinetics.

growth) will be estimated from experimental data using the relationships

$$\sigma_{Ln}^2 = \sigma_{Lf}^2 - \sigma_{Lo}^2 \tag{13}$$

$$\bar{L}_n = \bar{L}_f - \bar{L}_o \tag{14}$$

These experimental values will then be compared with similar quantities calculated assuming size-dependent growth to be the only factor in altering the distribution.

Regression of the σ_{Ln}^2 vs. $\bar{L}_n$ yields

$$\sigma_{Ln}^2 = 1.97\,\bar{L}_n^{1.35} \tag{15}$$

The correlation coefficient R is 0.973, and the 95% confidence limits are 1.55 to 2.50 on the proportionality coefficient, and ±0.10 on the order with respect to extent of growth. This equation is plotted in Figure 6 with the contribution to the size variance by size-dependent growth discussed below.

The potential contribution of size-dependent growth to the developing size dispersion can be estimated using Eq. 10. The average size of nuclei formed by initial breeding and the standard deviation of the nuclei population were determined in a study to be reported separately. For the 13 experiments analyzed, the crystals formed by initial breeding were estimated to have an average size of 5 μm with 95% of the crystals within ±2.7 μm of the average. The moment coefficient of kurtosis for this initial distribution was estimated to be twice that of a normal distribution, meaning that 95% of the initial population was within plus or minus one standard deviation as opposed to two standard deviations.

From the above description of the initial crystal population, 95% of all original crystals are between 2.3 and 7.7 μm in size; these limits will be denoted L_1' and L_2', respectively. Growth will increase the size of the 2.3 μm crystals to L_1'' and the size of the 7.7 μm crystals to L_2''. If the growth rates are exclusively size-dependent, and if this dependence is given by Eq. 10, then a growth period will result in 95% of all crystals in the distribution lying between L_1'' and L_2''. Moreover, the mean size $\bar{L}_f$ will be the average of these limits. As a_4 was found to decrease with $\bar{L}_n$, more than plus or minus one standard deviation σ_{Lf} will be required to encompass 95% of the crystals in the final distribution. Although this tends to overestimate σ_{Lf}^2, especially if growth rate is a strong function of size, $L_2'' - L_1''$ will be assumed to be equal to 2 σ_{Lf}. Once σ_{Lf}^2 is calculated, σ_{Ln}^2 is given by Eq. 13 where $\sigma_{Lo}^2 = 7.3\ \mu m^2$.

Substituting the definition of G (Eq. 5) into Eq. 10 gives

$$\Delta L_2/\Delta L_1 = (L_2/L_1)^{0.40} \tag{16}$$

where

$$\Delta L_2 = L_2'' - L_2' \tag{17}$$

$$\Delta L_1 = L_1'' - L_1' \tag{18}$$

Using the average sizes for the upper and lower limits of the distribution to account for the effect of size on growth, let

$$L_2 = (L_2'' + L_2')/2 \tag{19}$$

and

$$L_1 = (L_1'' + L_1')/2 \tag{20}$$

Substituting Eqs. 17–20 into Eq. 16 gives

$$[(L_2'' - L_2')/(L_1'' - L_1')] = [(L_2'' + L_2']/(L_1'' + L_1')]^{0.4} \tag{21}$$

Finally, substituting known values of L_1' and L_2' gives a relationship between L_1'' and L_2''. Once L_1'' and L_2'' are known, σ_{Ln}^2 and $\bar{L}_n$ can be calculated as described earlier. For a range of values of L_1'' corresponding values of L_2'' can be evaluated, and the relationship between σ_{Ln}^2 and $\bar{L}_n$ determined.

Correlating the dispersion of the distribution (as denoted by σ_L^2) with the advance of the distribution gave

$$\sigma_L^2(\mathrm{SDG}) = 2.49\,\bar{L}_n^{0.57} \tag{22}$$

where the potential size variance caused by size-dependent growth rates is denoted by (SDG). Equation 22 is plotted in Figure 6.

As shown in Figure 6, size-dependent growth can make only a minor contribution to the overall size variance of the developing crystal size distribution. This is because the original distribution is nearly monodisperse. The estimation of σ_L^2(SDG) is based on the assumption that growth is exclusively size-dependent, and that that size-dependency is given by Eq. 10. Since the size variance appears to be largely controlled by a growth rate dispersion, Eq. 10 must chiefly reflect *apparent* size-dependent growth, which, as has been discussed, results from the classification of crystals into sizes by their growth rates. Therefore, for small potassium alum crystals obtained by initial breeding, growth rate dispersion determines observed crystal growth; if size-dependent growth is present, it is masked by growth rate dispersion.

Seed Crystal Growth

Growth rate dispersion, as characterized by changes in size variance, was evaluated for the octahedral seed crystals in four experiments in which there was extensive seed growth. These data were obtained on the 250–300 μm and the 300–355 μm fractions. The original size variance σ_{Lo}^2 of the seed crystals was estimated by the equation

$$\sigma_{Lo}^2 = [(L_u - L_l)/2]^2 \tag{23}$$

The upper and lower sieve sizes bracketing the fractions from which the seed samples were taken are denoted L_u and L_l, respectively. These were adjacent sieves in the fourth root of two size progression series. The final size variance σ_{Lf}^2 of the distribu-

TABLE 2. DISPERSION PARAMETERS FOR LARGE POTASSIUM ALUM CRYSTAL DISTRIBUTIONS

Section No.	a_l–a_u* (μm)	$\bar{L}_o$ (μm)	$\bar{L}_f$ (μm)	σ^2_{Lo} (μm^2)	σ^2_{Lf} (μm^2)	σ^2_L (μm^2)	$\bar{L}$ (μm)
I	250–300	275	519	625	2,746	2,121	244
This Research	300–355	328	455	756	1,756	999	127
	300–355	328	442	756	1,832	1,076	114
	300–355	328	421	756	1,673	917	93
II	248–272	260	465	144	1,024	880	205
Janse and	248–272	260	464	144	1,024	880	204
DeJong (1979)	456–498	477	681	441	2,116	1,675	204
	456–498	477	663	441	1,296	855	186
	542–592	567	736	625	1,444	819	169
	456–498	477	636	441	1,681	1,240	159

* Original seed fraction before growth.

tion after growth was calculated by Eq. 2, and the variance due to growth $\sigma_{Ln}{}^2$ was obtained by Eq. 13.

The original mean size $\bar{L}_o$ of the seed size distribution was taken as a simple average of the upper and lower sieve mesh sizes bracketing the fraction. The final mean size $\bar{L}_f$ was calculated from experimental data using Eq. 1, and the extent of growth $\bar{L}_n$ was calculated from Eq. 14. Moments of the distributions before and after growth are summarized in Table 2, which compares data from this work with those of Janse and deJong (1979). The latter data were obtained from experiments at constant supersaturations and covered the supersaturation range from 0.092 to 0.097. These supersaturations are considerably higher than those in the present study, although temperatures in the two studies were identical.

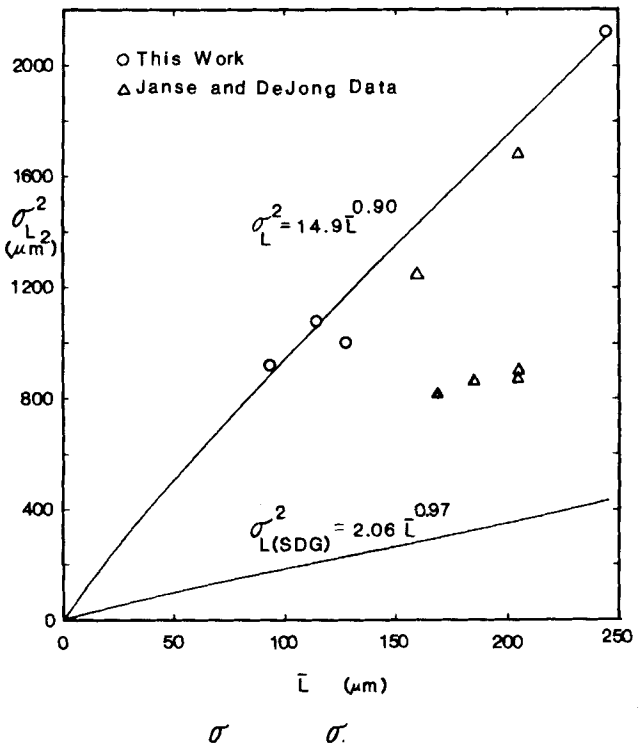

Figure 7. Comparison of dependence of size variance on extent of growth determined experimentally for large potassium alum crystals with that estimated assuming size-dependent growth kinetics.

The data from the present study were graphed in Figure 7, showing σ^2_{Ln} as a function of the extent of growth L_n. Correlation of these data yields

$$\sigma^2_{Ln} = 14.9\bar{L}_n^{0.90} \tag{24}$$

The correlation coefficient is 0.972; the 95% confidence limits on the constant are 0.6 to 368.3, and on the order they are ± 0.65. The uncertainties are substantial. The Janse and deJong data, also plotted in Figure 7, fall significantly below data from this study. This difference could be explained by the fact that their experiments used higher and constant supersaturations.

As was done for the nuclei formed by initial breeding, the possible contribution of size-dependent growth rates to the size variance $\sigma_L{}^2$(SDG) was determined. The same procedure was followed to calculate size variance for the large crystal distribution as was used for the small crystals. One hundred percent of the crystals were within $L_1' = 300$ and $L_2' = 355$ μm, the bracketing sieve sizes of the most frequently used seed fraction. $\bar{L}_o$ was 327.5 μm and $\sigma_{Lo}{}^2$ was 756.2 μm^2, as calculated by Eq. 23.

Values of $\sigma_L{}^2$(SDG) and $\bar{L}_n$ resulting from the above calculations were correlated by linear regression to obtain

$$\sigma^2_L(SDG) = 2.06\,\bar{L}_n^{0.97} \tag{25}$$

This correlation is plotted in Figure 7 for comparison with the overall measured size variance for large seed crystals. As can be seen, the final variance in seed size distribution, which is assumed to arise from an initial size spread of 55 μm, cannot account for the measured size variance or the growth behavior of the seed crystals. Again, it has been assumed in the estimation of $\sigma_L{}^2$(SDG) that crystal growth is exclusively size-dependent and growth rate is proportional to $L^{0.40}$. This hypothetical size-dependency of crystal growth rate does not explain the observed growth in the spread of the crystal size distribution, and if it exists at all, it is masked by the effects of growth rate dispersion.

The size variance and average growth rates of small and large crystals could not be compared meaningfully because the histories of the two populations were extremely different. Nothing was known about the original distribution from which the 250 to 355 μm seed fraction was obtained. Also, seed crystals were sieved and exposed to the atmosphere, which could have introduced surface dislocations or altered the average screw dislocation activity of these crystals. On a Knoop hardness scale, potassium alum has a value of about 45 (Tai et al., 1975) and brass, from which the sieves were made, has a hardness of 135 to 165 (Weast, 1973). Therefore, potassium alum is about four times softer than brass and could be deformed by the brass wire mesh.

ACKNOWLEDGMENT

Partial support of this research by the National Science Foundation, under Grant ENG-78-22656, is gratefully acknowledged.

NOTATION

a_4 = moment coefficient kurtosis
c = prevailing concentration of potassium alum
c^* = equilibrium concentration of potassium alum at the system temperature
G = crystal growth rate
$\bar{G}$ = advance rate of distribution mode
K_G = coefficient in Eq. 8
k_v = volume shape factor
L = crystal size or edge length
$\bar{L}$ = mean size
L_i = mean size of Coulter counter channel i
$\bar{L}_n$ = net growth or extent of growth, Eq. 14
L_s = diameter of a sphere
L_1' = lower size limit of a population before growth
L_1'' = lower size limit of a population after growth
L_2' = upper size limit of a population before growth
L_2'' = upper size limit of a population after growth
ΔL = displacement of fraction of oversize crystals
$\Delta \bar{L}$ = displacement of the mode of a distribution
m = mass of crystals
n = exponent relating growth rate and relative supersaturation
n_c = number of crystals in a distribution
N_i = number of crystals per unit slurry volume in channel i
Δt = time interval

Greek Letters

ϵ = screw dislocation activity in Burton-Cabrera-Frank model
ρ_c = crystal density
σ = relative supersaturation, $(c - c^*)/c^*$
σ_L = standard size deviation
σ_L^2 = size variance
σ_{Ln}^2 = net size variance due to growth, Eq. 13

Subscripts

f = final
o = original

LITERATURE CITED

Bennema, P., "Interpretation of the Relations Between the Rate of Crystal Growth from Solution and the Relative Supersaturation at Low Supersaturation," *J. Cryst. Growth*, **1**, 287 (1967).

Berglund, K. A., and M. A. Larson, "Growth of Contact Nuclei of Citric Acid Monohydrate," *AIChE Symp. Ser.*, **78**(215), 9 (1982).

———, "Modeling of Growth Rate Dispersion of Citric Acid Monohydrate in Continuous Crystallizers," *AIChE J.*, **30**, 280 (1984).

Bujac, P. D. B., "Attrition and Secondary Nucleation in Agitated Crystals Slurries," *Industrial Crystallization '75*, J. W. Mullin, Ed., Plenum Press, New York, 23 (1976).

Burton, W. K., N. Cabrera, and F. C. Frank, "The Growth of Crystals and the Equilibrium Structure of their Surfaces," *Phil. Trans. Roy. Soc.*, **243**(A866), 299 (1951).

Garside, J., "The Growth of Small Crystals," *Industrial Crystallization '78*, E. J. de Jong and S. J. Jancic, Eds., North-Holland, Amsterdam, 143 (1979).

Garside, J., and R. J. Davey, "Secondary Contact Nucleation: Kinetics, Growth and Scale-up," *Chem. Eng. Commun.*, **4**, 393 (1980).

Garside, J., and S. F. Jancic, "Growth and Dissolution of Potash Alum Crystals in the Subsieve Size Range," *AIChE J.*, **22**, 887 (1976).

———, "Measurement and Scale-Up of Secondary Nucleation Kinetics for the Potash Alum-Water System," *AIChE J.*, **25**, 948 (1979).

Garside, J., and M. A. Larson, "Direct Observation of Secondary Nuclei Production," *J. Cryst. Growth*, **43**, 694 (1978).

Garside, J., I. T. Rusli, and M. A. Larson, "Origin and Size Distribution of Secondary Nuclei," *AIChE J.*, **25**, 57 (1979).

Janse, A. H., and E. J. deJong, "The Occurrence of Growth Dispersion and Its Consequences," *Industrial Crystallization '75*, J. W. Mullin, Ed., Plenum Press, New York, 145 (1976).

———, "Growth and Growth Dispersion," *Industrial Crystallization '78*, E. J. deJong and S. J. Jancic, Eds., North-Holland, Amsterdam, 135 (1979).

McCabe, W. L., "Crystal Growth in Aqueous Solutions," *Ind. Eng. Chem.*,**21**, 30 (1929).

Misra, C., and E. T. White, "Kinetics of Crystallization of Aluminum Trihydroxide from Seeded Caustic Aluminate Solutions," *CEP Symp. Ser.*, **67**(110), 53 (1971).

Randolph, A. D., and E. T. White, "Modeling Size Dispersion in the Prediction of Crystal Size Distribution," *Chem. Eng. Sci.*, **32**, 1,067 (1977).

Rousseau, R. W., S. Craig, and W. L. McCabe, "Formation, Survival and Growth of Nuclei from Secondary Nucleation," *Industrial Crystallization '78*, E. J. deJong and S. J. Jancic, Eds., North-Holland, Amsterdam, 19 (1979).

Tai, C. Y., W. L. McCabe, and R. W. Rousseau, "Contact Nucleation of Various Crystal Types," *AIChE J.*, **21**, 351 (1975).

Van Enckevort, W. J. P., and W. H. Van der Linden, "On the Relation Between Etch Pits and Growth Hillocks and Dislocations on the (111) Faces of Potassium Aluminum Alum," *J. Cryst. Growth*, **47**, 196 (1979).

van't Land, C. M., and B. G. Wienk, "Control of Particle Size in Industrial NaCl Crystallization," *Industrial Crystallization '75*, J. W. Mullin, Ed., Plenum Press, New York, 51 (1976).

Weast, R. C., Ed., *Handbook of Chemistry and Physics*, 54th Ed., CRC Co., Cleveland, F18 (1973).

White, E. T., and P. G. Wright, "Magnitude of Size Dispersion Effects in Crystallization," *CEP Symp. Ser.*, **67**(110), 81 (1971).

Manuscript received June 4, 1984, Revision received Dec. 12, 1984, and accepted Jan. 8, 1985.